ChemPubSoc Europe

DOI: 10.1002/chem.201905310

CHEMISTRY A European Journal Full Paper

Hydrogels

Acid-Cleavable Poly(ethylene glycol) Hydrogels Displaying Protein Release at pH 5

Johannes Ewald,[a] Jan Blankenburg,[a, b] Matthias Worm,[a] Laura Besch,[c] Ronald E. Unger,[d] Wolfgang Tremel,[c] Holger Frey,*[a] and Hannah Pohlit*[a, e]

Abstract: PEG is the gold standard polymer for pharmaceutical applications, however it lacks degradability. Degradation under physiologically relevant pH as present in endolysosomes, cancerous and inflammatory tissues is crucial for many areas. The authors present anionic ring-opening copolymerization of ethylene oxide with 3,4-epoxy-1-butene (EPB) and subsequent modification to introduce acid-degradable vinyl ether groups as well as methacrylate (MA) units, enabling radical cross-linking. Copolymers with different molar ratios of EPB, molecular weights (M_n) up to 10 000 g mol^{-1} and narrow dispersities ($Đ < 1.05$) were prepared. Both the P(EG-*co*-*iso*EPB)MA copolymer and the hydrogels showed pH-dependent, rapid hydrolysis at pH 5–6 and long-term storage stability at neutral pH (pH 7.4). By designing the degree of polymerization and content of degradable vinyl ether groups, the release time of an entrapped protein OVA-Alexa488 can be tailored from a few hours to several days (hydrolysis half-life time $t_{1/2}$ at pH 5: 13 h to 51 h).

Introduction

Poly(ethylene glycol) (PEG) is a biocompatible, water-soluble polymer used for cosmetics, pharmaceutics and medical applications.[1] Due to its low immunogenicity, antigenicity and toxicity, the bioconjugation of protein drugs with PEG (known as "PEGylation") is the established gold standard employed to modify therapeutic molecules like peptides, proteins or aptamers.[2] Furthermore, PEG is used extensively as a hydrogel scaffold for the controlled release of biomolecules[3] or cells[4] in regenerative medicine.[5] The PEG delivery vehicles take advantage of the versatility of the PEG chemistry that allows for a tailored design of the required hydrogel properties. Although mechanical[6] and biological properties[7] as well as hydrogel porosity[8] can be optimized independently, adjusting the degradability without altering the aforementioned properties remains a challenge. In general, PEG hydrogels lack degradability under physiological conditions within relevant time spans. Hydrogels derived from traditional diacrylated PEG (PEGDA) are hydrolyzed slowly and unspecifically in vivo, which renders them unsuitable for long-term storage as well as for implantable applications.[9] Therefore, the use of nondegradable PEG molecules larger than 30 kDa for medical applications is limited because these cannot be excreted by the kidney due to the kidney-threshold and may accumulate in the tissue.[10] However, the use of hydrogels composed of high molecular weight PEG chains would result in larger average pore size and greater swelling ability of the gel, which is thought to be favorable for the release of larger therapeutic molecules depending solely on diffusion[11] like antibodies. This approach can be advantageous when considering a constant diffusive release. Alternatively, acid-triggered controlled release combined with advanced storage stability is typical for hydrogels from shorter, degradable PEG chains eliminating unspecific drug release depending solely on diffusion. This may open a new range of applications for the use of PEG hydrogels for in vivo applications, for example, degradable injectable hydrogels, micro- or nanosized delivery vehicles, wound-healing hydrogel patches, and directed drug delivery for tumor treatment.

In this context, considerable efforts have been devoted to synthesize intrinsically cleavable PEGs that respond to environ-

[a] J. Ewald, Dr. J. Blankenburg, Dr. M. Worm, Prof. H. Frey, Dr. H. Pohlit
Institute of Organic Chemistry, Johannes Gutenberg-University
Duesbergweg 10–14, 55128 Mainz (Germany)
E-mail: hfrey@uni-mainz.de

[b] Dr. J. Blankenburg
Graduate School Materials Science in Mainz
Staudinger Weg 9, 55128 Mainz (Germany)

[c] L. Besch, Prof. W. Tremel
Institute of Inorganic Chemistry and Analytical Chemistry
Johannes Gutenberg-University, Duesbergweg 10–14
55128 Mainz (Germany)

[d] Dr. R. E. Unger
Institute for Pathology, Johannes Gutenberg University Mainz
Obere Zahlbacher Straße 63, 55101 Mainz (Germany)

[e] Dr. H. Pohlit
Engineering Sciences Department, Science for Life Laboratory
Uppsala University, Lägerhyddsvägen 1, 75121 Uppsala (Sweden)
E-mail: hannah.pohlit@angstrom.uu.se

Supporting information and the ORCID identification number(s) for the author(s) of this article can be found under: https://doi.org/10.1002/chem.201905310.

mental stimuli.[1,12] Polymer cleavability in acidic environment as found intracellularly inside the endolysosome,[13] in inflamed tissue,[11a,14] tumor tissue,[15] or vaginal tissue[16] can be achieved by inserting acid-labile moieties.[17] Various innovative approaches for introduction of acid-degradable functional groups into a polyether backbone were reported. These strategies include step-growth polymerization, oxidation, or copolymerization with epichlorohydrin or lactide, or by introducing acetals,[18] ketals,[19] hydrazones,[20] *cis*-acetonitic acids,[21] maleamic acid derivatives,[22] imines,[23] β-thiopropionates,[24] or esters.[25] However, these strategies generate either polydisperse materials or polymers with ill-defined end-groups.[26] The availability of nearly monodisperse, high molecular weight PEGs with acid-labile vinyl ether degradation sites has the potential to open up a vast range of applications using PEG hydrogels in vivo. Here, we present well-defined PEG building blocks with cross-linkable end groups that degrade at physiologically relevant pH in practicable time scales, while preserving long-term storage stability. Furthermore, we demonstrate that the size of the nontoxic degradation products can be tailored by customizing the number of degradable vinyl ether units per polymer chain.

Results and Discussion

Synthesis

Recently, we established the synthesis of multi allyl ether-functional PEG by anionic ring-opening copolymerization of ethylene oxide (EO) and 3,4-epoxy-1-butene (EPB).[27] Copolymerization of EPB and EO was performed in a DMSO/THF mixture at room temperature by using sodium hydride as a base (see Scheme 1).

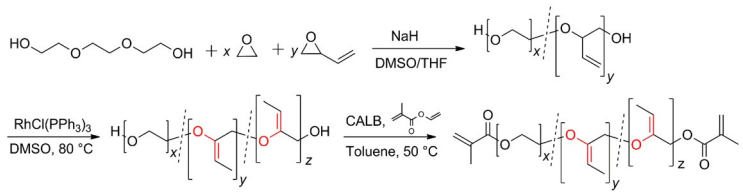

Scheme 1. Copolymerization of EO and EPB as well as post-polymerization isomerization and methacrylate derivatization.

We use triethylene glycol as a bifunctional initiator resulting in well-defined P(EG-*co*-EPB) copolymers ($Đ = 1.03–1.05$) with adjustable EPB content (5–10 mol%) and molecular weight (5000–10000 g mol^{-1}, see Table 1). Isomerization of the allyl moieties with Wilkinson's catalyst $RhCl(PPh_3)_3$ results in vinyl ethers (*iso*EPB) that exhibit fast hydrolysis in slightly acidic conditions, while being long-term stable under neutral conditions.[27] In the final step, methacrylate units are attached to the degradable polymers using an enzyme-catalyzed, mild esterification reaction. The latter simple modification enables radical crosslinking of the PEG copolymer building block to degradable hydrogels that are suitable for drug delivery and controlled release.

Characterization

All synthesized copolymers were characterized by ^{1}H NMR, size exclusion chromatography (SEC) and mass spectrometry (MALDI-ToF). Exemplarily, the data of P(EG_{168}-*co*-EPB_{13}) and its derivatives are discussed in the main text. Extensive analytical data of the other polymers can be found in the Supporting Information. Molecular weights were calculated from ^{1}H NMR spectra by comparing the signals of the ethylene oxide polymer backbone with the signal of the hydroxyl units. The percentage of EPB incorporation was calculated by comparing the integrals of the allyl NMR signals at 5.84 ppm and 5.74 ppm (EPB) or the vinyl NMR signal at 4.78 ppm (*iso*EPB) with the signal of the two hydroxyl end-groups at 4.6 ppm. Isomerization with Wilkinson's catalyst resulted in the disappearance of the EPB signals between 6.0 and 5.2 ppm and the appearance of the vinyl ether signals at 4.8–4.5 ppm (see Figure S19, Supporting Information). SEC underestimates the actual molecular weights because of the different hydrodynamic volume of the copolymer that is compared to the PEG standard used for SEC calibration. All SEC traces showed monomodal molecular weight distributions, and molecular weights did not change significantly upon post-polymerization functionalization. A typical ^{1}H NMR spectrum of P(EG-*co*-*iso*EPB)MA is given in Figure 1a. SEC traces of P(EG_{168}-*co*-EPB_{13}) copolymer and its derivatives are presented in Figure 1b. MALDI-ToF was performed to confirm that all polymers were initiated from triethylene glycol and to confirm copolymeriza-

Table 1. Molecular characteristics of P(EG-*co*-EPB) copolymers and of post-polymerization modified copolymers.

Sample	After isomerization				After methacrylation				After hydrolysis							
	M_n[a]	mol% EPB[b]	M_n[c]	$Đ$[d]	M_n[a]	mol% EPB[b]	M_n[c]	$Đ$[d]	M_n[a]	mol% EPB[b]	M_n[c]	$Đ$[d]	M_n[c]	$Đ$	$t_{1/2}$[e] at pH 4	$t_{1/2}$[e] at pH 5
P(EG_{112}-*co*-EPB_5)	5150	5	3730	1.03	5280	5	3720	1.03	5280	5	3700	1.03	880	1.75	4.5 h	51 h
P(EG_{202}-*co*-EPB_9)	9310	5	6950	1.03	9540	5	6730	1.04	9540	4	6690	1.03	830	1.85	3.6 h	15 h
P(EG_{113}-*co*-EPB_9)	5410	10	3620	1.03	5620	8	3580	1.05	5640	8	3600	1.05	670	1.55	2.3 h	14 h
P(EG_{168}-*co*-EPB_{13})	7970	9	6420	1.03	8280	8	6360	1.03	8280	7	6190	1.04	900	1.94	2.3 h	13 h

M_n = expressed in [g mol^{-1}]. [a] Determined by NMR [400 MHz, [D_6]DMSO].; [b] mol% EPB: content of EPB calculated from ^{1}H NMR spectra; [c] determined by SEC (DMF, PEG standards, RI signal); [d] $Đ = M_w/M_n$: dispersity of polymer samples (SEC); [e] $t_{1/2}$ = hydrolysis half-life time, determined by on-line absorbance measurements.

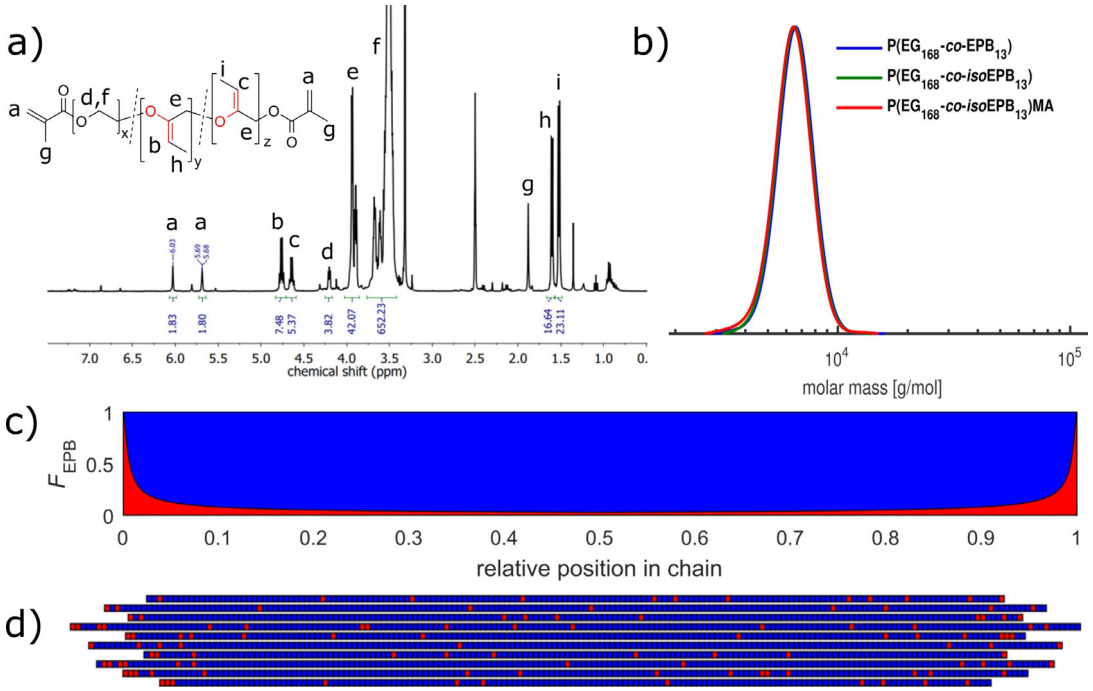

Figure 1. Polymer analytics of representative copolymer P(EG_{168}-*co*-EPB_{13}). a) ^{1}H NMR spectrum (400 MHz, [D_6]DMSO). b) SEC traces (DMF, PEG standards, RI signal) of synthesized copolymer and after subsequent post-polymerization reactions. c) Gradient of EPB units along the copolymer chain polymerized from bifunctional initiator based on the determined reactivity ratios, blue: ethylene oxide, red: EPB. d) Sampling of ten individual copolymer chains obtained by Monte Carlo simulation performed for the polymer composition P(EG_{168}-*co*-EPB_{13}) initiated from triethylene glycol and is based on the determined reactivity ratios.

tion of EPB and EO (Figures S5 and S11, Supporting Information).

To comprehend the monomer sequence distribution during anionic ring-opening copolymerization, on-line ^{1}H NMR measurements—a technique that has been proven extremely useful to monitor polymerization reactions in situ[28]—has been employed during copolymerization of EPB and EO. The reactivity ratios were determined by fitting the in situ data to the ideal copolymerization model to be $r_{EPB} = 0.35$ and $r_{EO} = 2.8$ (Figure S33, Supporting Information).[29]

The results were confirmed by classical aliquot taking at determined points in time from the bulk polymerization reaction. Based on these reactivity ratios the average microstructure was depicted for a copolymer started by a bifunctional initiator with the same composition as P(EG_{168}-*co*-EPB_{13}), see Figure 1c. Individual copolymer chains obtained by a Monte Carlo simulation carried out for the composition of P(EG_{168}-*co*-EPB_{13}), based on the determined reactivity ratios and living polymerization behavior, are displayed in Figure 1d. Incorporation of EPB moieties results in a gradient microstructure with higher ratio of EPB at the termini of the polymer chains and lower EPB content near the bifunctional initiator.

To investigate the biocompatibility of the polymer to cells, in vitro cell studies with MG-63 and primary HUVEC cells were conducted. A solution of 50–500 μg mL^{-1} P(EG_{92}-*co*-*iso*EPB_6) was added to the cell culture and vitality staining with Calcein-AM was performed after 24 h, 72 h and 7 days. For MG-63 cells, no difference compared to the untreated control cells was detected upon incubation of 500 μg mL^{-1} P(EG_{92}-*co*-*iso*EPB_6) after 7 days of culture. For primary HUVEC cells, only for the highest concentration of 500 μg mL^{-1} tested, P(EG_{92}-*co*-*iso*EPB_6) showed diminished cell survival after 72 h of cell culture. For 100 μg mL^{-1}, no difference compared to the untreated control cells was observed.

Macromonomer degradation

The vinyl ether units within the P(EG-*co*-*iso*EPB)MA polymer backbone are susceptible to hydrolysis upon acidification (see Figure 2a, bottom). The macromonomers break down completely upon incubation with dilute HCl overnight. Subsequently, base was added to adjust the pH above 3, and degradation fragments were analyzed by SEC (representative elution trace is displayed in Figure 2a, top). Half-life degradation times for hydrolysis were determined with ^{1}H NMR, as described previously[27] (Table 1). The EPB content was tailored to give degradation products of 670–900 g mol^{-1}, which allow for renal excretion. The degradation behavior can be predicted by the Monte Carlo simulation shown in Figure S26 (Supporting Information). In the simulated degradation of P(EG_{168}-*co*-EPB_{13}) the PEG-fragments show a very similar size distribution to that obtained experimentally.

Hydrogel synthesis, degradation and protein release

To obtain a hydrogel, 10 wt% P(EG-*co*-*iso*EPB)MA solutions were mixed with 2-hydroxy-4′-(2-hydroxyethoxy)-2-methylpropiophenone (photoinitiator in ethanolic solution (1:10)) and

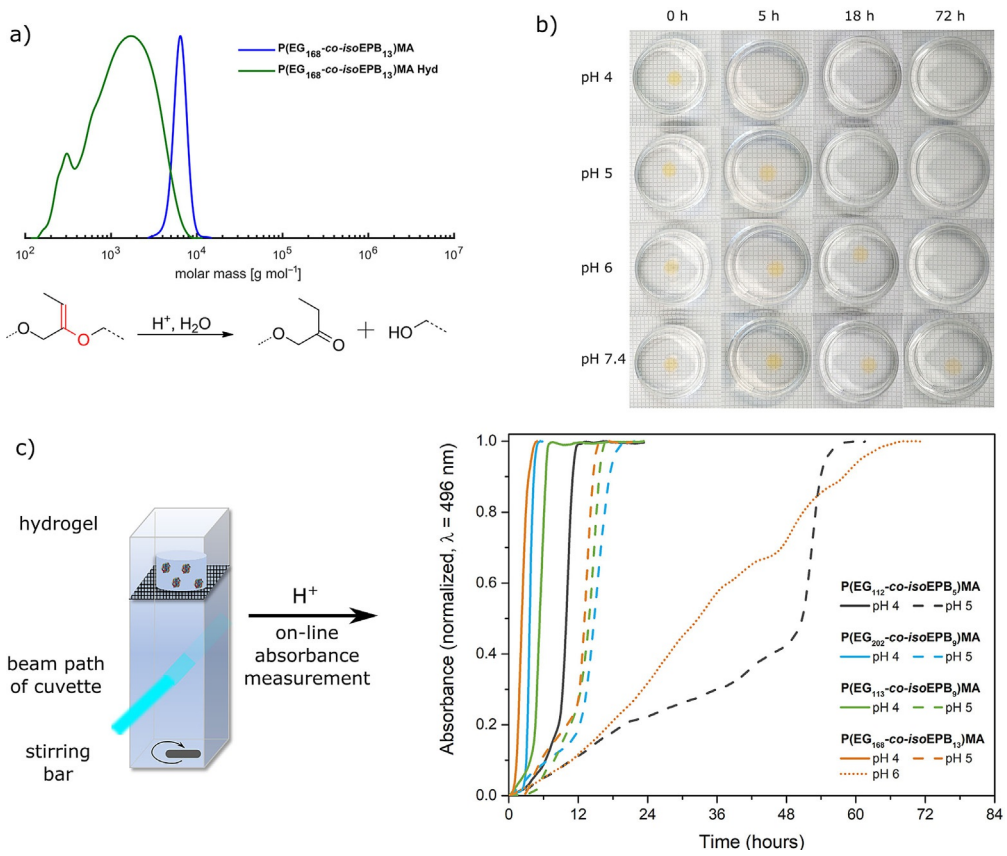

Figure 2. Hydrogel degradation and protein release a) SEC traces (DMF, PEG standards, RI signal) of P(EG_{168}-*co*-EPB_{13})MA before and after hydrolysis. Bottom: Reaction scheme of hydrolysis of vinyl ether moieties in copolymer chain at acidic pH. b) Photographs of the degradation of OVA-Alexa488 loaded hydrogels from P(EG_{168}-*co*-*iso*EPB_{13})MA incubated at different pH over 72 h at room temperature. c) (left) Scheme of experimental setup for on-line absorbance measurements of OVA-Alexa488 release kinetics from hydrogel composed of P(EG_{168}-*co*-*iso*EPB_{13})MA in cuvette at different pH values; (right) on-line absorbance measurements of OVA-Alexa488 release kinetics from hydrogels prepared from copolymers with different molecular weight and different EPB content (pH 4 and pH 5).

cross-linked for 15 min, by using a 365 nm UV lamp and a 96 well plate at pH 7.4. Employing this composition results in transparent hydrogels with defined edges that hold the shape of the mold well. Furthermore, the good mechanical stability of the hydrogels allows for easy handling with tweezers. To help monitoring the hydrogel degradation during macroscopic degradation studies with the unaided eye, the gel was loaded with the dye labelled model protein OVA-Alexa488. This results in transparent yellowish gels (Figure 2b). Hydrogel disks from copolymer P(EG_{168}-*co*-*iso*EPB_{13})MA were incubated in a phosphate-citrate buffer at pH 4, 5 or 6 or phosphate buffer at pH 7.4 as a control (compare Figure 2b). The plastic Petri dishes containing the buffer solution and hydrogel were incubated at room temperature. The control hydrogel at pH 7.4 remained unchanged for periods exceeding 5 days, whereas the hydrogel incubated at pH 4 disintegrated within 5 hours, the hydrogel at pH 5 within 18 hours and the hydrogel at pH 6 within 72 hours. These results demonstrate that 10 wt% hydrogels comprising the synthesized P(EG_{168}-*co*-*iso*EPB_{13})MA macromonomer degraded quickly under physiological conditions of pH 5–6, as found in the endolysosome or inflamed tissue while being stable when stored in neutral solutions for several months (data not shown). It should be noted that the proton diffusion occurs on much shorter time scales than those of the observed degradation and OVA-Alexa 488 release of the hydrogels. This proves that the polymer hydrolysis is location-independent and takes place in the entire gel simultaneously (see Figure S38, Supporting Information). This shows that hydrogels can be perfused with small molecules for possible application as a bioreactor when enzymatically active proteins are encapsulated in the hydrogel. Furthermore, the protein release from a 10 wt% P(EG-*co*-*iso*EPB)MA hydrogel was investigated by using absorbance measurements at 496 nm in a disposable PMMA cuvette. To ensure that the change in absorbance measured arose exclusively from the released protein and not from the protein encapsulated in the hydrogel, a cuvette with an incubation chamber for the hydrogel with spatial separation from the absorbance beam path was designed (see Figure 2c, left and Figure S34, Supporting Information). The acidified buffer solution was stirred constantly with a magnetic stir bar, while the absorbance was measured every 5 minutes until the absorbance signal remained constant. Incubation of the hydrogel in more acidic buffer solution resulted in faster degradation (see Figure 2c), whereas incubation at neutral pH did not lead to significant release over the same period of time. We normalized the absorbance values of hydrogels prepared from differ-

ent macromonomers and degraded at different pH, since the absorbance of OVA-Alexa488 differs with pH. Three trends can be observed: 1) The lower the pH, the faster hydrogel degradation and consequently protein release take place. 2) In addition, with increasing content of degradable vinyl ether units in the macromonomers, the degradation rate increases. 3) The highest degradation rate was observed for the hydrogel composed of the largest macromonomer with high EPB molar content. Alternatively, the lowest degradation rates are observed for the smallest macromonomer with low EPB content under otherwise similar conditions.

These findings can be rationalized by considering network density, which determines protein diffusion. As shown in Figure 2c, the protein release rate from the networks increases once a few isoEPB units are cleaved. In case of slow release of OVA-Alexa488, the absence of an initial burst release is observed. When the protein-loaded hydrogels are incubated first at neutral pH (pH 7.4), the protein release reaches a plateau once the surface-adsorbed protein is released (see Figures S28 and S35, Supporting Information). Subsequent transfer of the hydrogel into a slightly more acidic solution (pH 6) results in continued protein release. Similar behavior is visible for the network obtained from the smallest copolymer P(EG_{112}-*co*-*iso*EPB_5) incubated at pH 5, for which the densely cross-linked hydrogel in the beginning only allows surface-adsorbed OVA-Alexa488 to be washed out. After a certain period of time, a critical amount of *iso*EPB units is cleaved to open up larger pores for OVA-Alexa488 to diffuse out of the hydrogel. This trend can be observed both at pH 4 and at pH 5.

The hydrolysis half-life time ($t_{1/2}$) at pH 4 ranges from 2.3 to 4.5 hours and at pH 5 from 13 to 51 hours, depending on the copolymer employed (see Table 1). The P(EG_{168}-*co*-*iso*EPB_{13})MA macromonomer [$t_{1/2}$ (pH 5) = 13 h] is superior to previously published PEG-acetal macromonomers that required much longer time for degradation at physiological relevant pH values [$t_{1/2}$ (pH 5) = 48 h].[30] Likewise, it outperforms ketal-PEG macromonomers that degrade very quickly at acidic pH, but are not stable in neutral solutions, impeding storage for prolonged periods.[31]

The degradation behavior of a hydrogel consisting of the copolymer P(EG_{168}-*co*-*iso*EPB_{13}) is investigated by straightforward incubation at different pH values as well as by on-line absorbance release kinetics of entrapped OVA-Alexa488 (Figure 2b,c). Timescales of the hydrogel degradation behavior obtained by the two different methods are in good correlation, confirming these results.

In general, significant protein release (OVA-Alexa488, 45 kDa) from a nondegradable hydrogel of 10 wt% PEG with molecular weights of approximately 6000 Da does not occur.[32] This together with the fact that we cannot see a significant protein release of the hydrogel based on the largest macromonomer at pH 7.4 (compare Figure S27), but a remarkable release at pH 4, 5 and 6 evidences that the protein release from the hydrogels depends solely on acid stimuli and is not due to diffusion.

Conclusions

In summary, we have developed a new acid-degradable PEG hydrogel for pH-controlled degradation and protein release. Anionic ring-opening copolymerization of ethylene oxide and 3,4-epoxy-1-butene (EPB) allows for the precise adjustment of molecular weights and determines the content of degradable units within the polyether chains in the network. The reaction yields well-defined P(EG-*co*-EPB) copolymers with molecular weights from 5000 to 10000 g mol^{-1} (dispersities $Đ$ below 1.05) and high or low EPB content. Mild enzymatic conditions have been employed to obtain cross-linkable and degradable P(EG-*co*-*iso*EPB) methacrylate macromonomers. The highly water-soluble macromonomers readily degrade at physiologically relevant pH (pH 5–6) present in endolysosomes, inflammatory and cancerous tissue, while being stable for several weeks in solution at neutral pH (pH 7.4). Hydrogels prepared from the new macromonomers degrade macroscopically within 5 hours (pH 4), 18 hours (pH 5) or 72 hours (pH 6). The release of an encapsulated protein OVA-Alexa488 was monitored using a custom-designed release setup for on-line absorbance measurements and lasted between 13 hours for the hydrogel from the largest macromonomer with high EPB content to 51 hours for the hydrogel from the smallest macromonomer with low EPB content at pH 5. As expected, the hydrogels release the protein faster in more acidic buffer (pH 4, 2.3–4.5 hours) compared to less acidic conditions (pH 5, 13–51 hours). In neutral pH, no significant protein release can be detected.

The presented synthetic strategy paves the way for a new type of PEG hydrogel that combines the outstanding properties of PEG as a hydrogel constituent (e.g., biocompatibility, water-solubility and low immunogenicity) with degradation at physiologically relevant pH. To the best of our knowledge, long-term storage stability at pH 7.4 in combination with degradation at pH 6 reflects a uniquely precise pH sensitivity. In that respect, the concept also offers great potential for degradable PEG hydrogel nanocarriers.[30]

Experimental Section

Polymerization of P(EG-*co*-EPB)

The procedure is exemplarily described for the synthesis of copolymer P(EG_{168}-*co*-EPB_{13}). It was carried out similarly for all P(EG-*co*-EPB) copolymers presented in this paper. Sodium hydride (7 mg, 0.31 mmol) was transferred into a dry Schlenk flask and a solution of triethylene glycol (117 mg, 0.778 mmol) in benzene (6 mL) was added. The solution was stirred under slightly reduced pressure at 60 °C for 30 min keeping the stopcock closed. Moisture was removed by azeotropic distillation of benzene and subsequent drying at 60 °C in high vacuum for 16 h. After cooling to RT, dry THF (4 mL) was cryo-transferred into the Schlenk flask to dissolve the initiator. EPB (1.44 mL, 17.9 mmol, stirred over CaH_2 for 30 min and freshly distilled prior to use) and dry DMSO (7 mL) were injected into the Schlenk flask by using a syringe at −80 °C. Ethylene oxide (5 mL, 0.11 mol) was cryo-transferred with a graduated ampule, and the polymerization was proceeded at RT for 7 days and was subsequently quenched with methanol (2 mL). After dialy-

sis against methanol for 24 h (MWCO 1000 Da), the polymer was dried in vacuo (yield: 80%). ^{1}H NMR (400 MHz, [D$_6$]DMSO): $\delta = 5.72$ (ddd, 15.6 H, $^3J_{AB} = 17.2$ Hz, $^3J_{AB} = 10.5$ Hz, $^3J_{AB} = 6.7$ Hz, –CH=CH$_2$), 5.26 (m, 32.4 H, $^3J_{AB} = 17.2$ Hz, $^3J_{AB} = 2.1$ Hz, $^3J_{AB} = 1.1$ Hz, –CH=H*H*), 4.76 (q, 0.92 H, $J = 6.7$ Hz, C=C*H*–CH$_3$ (*E* isomer)), 4.57 (bs, 2 H, O*H*), 3.96–3.87 (m, 19.48 H, C*H*O–CH=CH$_2$, OC*H*$_2$–C=CH–CH$_3$ and C*H*$_2$O–C=CH–CH$_3$), 3.71–3.35 (m, 732 H, C*H*$_2$O), 1.52 ppm (d, 3.05 H, $J = 6.7$ Hz, C=CH-C*H*$_3$ (*E* isomer))

Isomerization of P(EG-*co*-EPB) to P(EG-*co-iso*EPB)

The procedure is exemplarily described for the synthesis of copolymer P(EG$_{168}$-*co-iso*EPB$_{13}$). The procedure was used accordingly for all P(EG-*co-iso*EPB) copolymers presented in this paper. In a Schlenk tube, P(EG$_{168}$-*co*-EPB$_{13}$) (800 mg, 0.10 mmol) was dissolved in DMSO and subjected to two freeze–pump–thaw cycles. Under argon atmosphere, RhCl(PPh$_3$)$_3$ (25 mg, 0.0275 mmol) was added and the solution was thoroughly degassed through two additional freeze–pump–thaw cycles. The light orange solution was stirred at 80 °C for one day and was twice precipitated in acetone/diethyl ether (1:1). The purified copolymer was obtained after drying in vacuum (yield: 94%). Isomerized copolymers were routinely stored in a refrigerator at 4 °C. ^{1}H NMR (400 MHz, [D$_6$]DMSO): $\delta = 4.77$ (q, 7.46 H, $J = 6.7$ Hz, C=C*H*–CH$_3$ (*E* isomer)), 4.65 (q, 5.28 H, $J = 6.7$ Hz, C=C*H*–CH$_3$ (*E* isomer)), 4.57 (bs, 1.48 H, O*H*), 3.99–3.88 (m, 42.02 H, OC*H*$_2$–C=CH–CH$_3$ and C*H*$_2$O–C=CH–CH$_3$), 3.71–3.35 (m, 655 H, C*H*$_2$O), 1.61 (d, 16.7 H, $J = 6.7$ Hz, C=CH–C*H*$_3$ (Z isomer)), 1.52 ppm (d, 23 H, $J = 6.7$ Hz, C=CH–C*H*$_3$ (*E* isomer)).

Methacrylation of P(EG-*co-iso*EPB) to P(EG-*co-iso*EPB)MA

The procedure is exemplarily described for the synthesis of copolymer P(EG$_{168}$-*co-iso*EPB$_{13}$)MA. The procedure was used accordingly for all P(EG-*co-iso*EPB)MA copolymers presented in this paper. In a Schlenk tube, P(EG$_{168}$-*co-iso*EPB$_{13}$) (400 mg, 0.05 mmol) was dissolved in toluene and CALB (30 mg) and vinyl methacrylate (60 μL, 0.50 mmol) were added. After stirring for 24 hours at 40 °C, the mixture was filtered, concentrated in vacuum and precipitated twice in diethyl ether. BHT was added as a stabilizer to prevent unwanted crosslinking and the polymer was dried in vacuum (yield 85%). ^{1}H NMR (400 MHz, [D$_6$]DMSO): $\delta = 6.04$ (s, 1.89 H, *H*$_2$C=CCH$_3$–C=O), 5.70 (s, 1.83 H, *H*$_2$C=CCH$_3$–C=O)4.77 (q, 7.26 H, $J = 6.7$ Hz, C=C*H*–CH$_3$ (*E* isomer)), 4.65 (q, 5.09 H, $J = 6.7$ Hz, C=C*H*–CH$_3$ (*E* isomer)), 3.99–3.88 (m, 40.75 H, OC*H*$_2$–C=CH–CH$_3$ and C*H*$_2$O–C=CH–CH$_3$), 3.71–3.35 (m, 655 H, C*H*$_2$O), 1.88 (s, 5.99 H, H$_2$C=CC*H*$_3$–C=O) 1.61 (d, 16.7 H, $J = 6.7$ Hz, C=CH–C*H*$_3$ (*Z* isomer)), 1.52 ppm (d, 23 H, $J = 6.7$ Hz, C=CH–C*H*$_3$ (*E* isomer)). ^{13}C NMR (100.6 MHz, [D$_6$]DMSO): $\delta = 152.40$ (1C, OCH$_2$–*C*=CH–CH$_3$ (*Z* isomer)) 150.62 (1C, OCH$_2$–C=*C*H–CH$_3$ (*E* isomer)), 135.81 (1C, CO–*C*=CH$_2$CH$_3$), 125.81 (1C, CO–C=CH$_2$CH$_3$), 106.35 (1C, C=CH–CH$_3$ (*E* isomer)), 96.13 (1C, C=CH–CH$_3$ (*Z* isomer)), 73.21–67.29 (48C, *C*H2O), 63.77 (1C, *C*O–C=CH$_2$CH$_3$), 17.97 (CO–C=CH$_2$*C*H$_3$), 11.34 (1C, C=C–CH$_3$ (*Z* isomer)) 9.95 ppm (1C, C=CH–*C*H$_3$ (*E* isomer)).

Additional experimental details (materials and methods and characterization data) can be found in the Supporting Information.

Acknowledgements

J.B. acknowledges a fellowship through the Excellence Initiative (DFG/ GSC 266) in the context of the graduate school MAINZ "Materials Science in Mainz". J.E. is grateful for an associate fellowship at the Mainz Research School of Translational Biomedicine (TransMed). The authors gratefully acknowledge the support of this research by Dr. Elena Berger-Nicoletti and Monika Schmelzer, who provided valuable polymer characterization.

Conflict of interest

The authors declare no conflict of interest.

Keywords: copolymerization · drug delivery · hydrogels · PEG · protein release

[1] J. Herzberger, K. Niederer, H. Pohlit, J. Seiwert, M. Worm, F. R. Wurm, H. Frey, *Chem. Rev.* **2016**, *116*, 2170 – 2243.
[2] K. Knop, R. Hoogenboom, D. Fischer, U. S. Schubert, *Angew. Chem. Int. Ed.* **2010**, *49*, 6288 – 6308; *Angew. Chem.* **2010**, *122*, 6430 – 6452.
[3] a) C. C. Lin, K. S. Anseth, *Pharm. Res.* **2009**, *26*, 631 – 643; b) T. Vermonden, R. Censi, W. E. Hennink, *Chem. Rev.* **2012**, *112*, 2853 – 2888.
[4] C. R. Nuttelman, M. A. Rice, A. E. Rydholm, C. N. Salinas, D. N. Shah, K. S. Anseth, *Prog. Polym. Sci.* **2008**, *33*, 167 – 179.
[5] B. V. Slaughter, S. S. Khurshid, O. Z. Fisher, A. Khademhosseini, N. A. Peppas, *Adv. Mater.* **2009**, *21*, 3307 – 3329.
[6] B. D. Polizzotti, B. D. Fairbanks, K. S. Anseth, *Biomacromolecules* **2008**, *9*, 1084 – 1087.
[7] J. Zhu, *Biomaterials* **2010**, *31*, 4639 – 4656.
[8] a) E. G. Gacasan, R. M. Sehnert, D. A. Ehrhardt, M. A. Grunlan, *Macromol. Mater. Eng.* **2017**, *302*, 1600512; b) A. Sannino, P. A. Netti, M. Madaghiele, V. Coccoli, A. Luciani, A. Maffezzoli, L. Nicolais, *J. Biomed. Mater. Res. Part A* **2006**, *79*, 229 – 236.
[9] M. B. Browning, S. N. Cereceres, P. T. Luong, E. M. Cosgriff-Hernandez, *J. Biomed. Mater. Res. Part A* **2014**, *102*, 4244 – 4251.
[10] a) P. Caliceti, *Adv. Drug Delivery Rev.* **2003**, *55*, 1261 – 1277; b) E. Markovsky, H. Baabur-Cohen, A. Eldar-Boock, L. Omer, G. Tiram, S. Ferber, P. Ofek, D. Polyak, A. Scomparin, R. Satchi-Fainaro, *J. Controlled Release* **2012**, *161*, 446 – 460.
[11] a) X. Yu, Q. Pan, Z. Zheng, Y. Chen, Y. Chen, S. Weng, L. Huang, *RSC Adv.* **2018**, *8*, 37424 – 37432; b) A. Bertz, S. Wohl-Bruhn, S. Miethe, B. Tiersch, J. Koetz, M. Hust, H. Bunjes, H. Menzel, *J. Biotechnol.* **2013**, *163*, 243 – 249; c) G. M. Cruise, D. S. Scharp, J. A. Hubbell, *Biomaterials* **1998**, *19*, 1287 – 1294.
[12] a) S. J. Buwalda, T. Vermonden, W. E. Hennink, *Biomacromolecules* **2017**, *18*, 316 – 330; b) S. Deshayes, A. M. Kasko, *J. Polym. Sci. Part A* **2013**, *51*, 3531 – 3566.
[13] a) N. Demaurex, *Physiology* **2002**, *17*, 1 – 5; b) H. Sun, T. L. Andresen, R. V. Benjaminsen, K. Almdal, *J. Biomed. Nanotechnol.* **2009**, *5*, 676 – 682; c) A. Asokan, M. J. Cho, *J. Pharm. Sci.* **2002**, *91*, 903 – 913.
[14] S. Guragain, B. P. Bastakoti, V. Malgras, K. Nakashima, Y. Yamauchi, *Chem. Eur. J.* **2015**, *21*, 13164 – 13174.
[15] a) P. Vaupel, F. Kallinowski, P. Okunieff, *Cancer Res.* **1989**, *49*, 6449 – 6465; b) N. R. Patel, B. S. Pattni, A. H. Abouzeid, V. P. Torchilin, *Adv. Drug Delivery Rev.* **2013**, *65*, 1748 – 1762; c) E. S. Lee, Z. Gao, Y. H. Bae, *J. Controlled Release* **2008**, *132*, 164 – 170.
[16] a) X. Sun, H. Qiu, Y. Jin, *Int. J. Pharm.* **2017**, *525*, 175 – 182; b) E. L. Larkin, L. Long, N. Isham, K. Borroto-Esoda, S. Barat, D. Angulo, S. Wring, M. Ghannoum, *Antimicrob. Agents Chemother.* **2019**, *63*, e02611 – e02618.
[17] P. Gupta, K. Vermani, S. Garg, *Drug Discovery Today* **2002**, *7*, 569 – 579.
[18] a) R. Tomlinson, J. Heller, S. Brocchini, R. Duncan, *Bioconjugate Chem.* **2003**, *14*, 1096 – 1106; b) E. R. Gillies, J. M. J. Fréchet, *Bioconjugate Chem.* **2005**, *16*, 361 – 368.
[19] a) S. Kim, O. Linker, K. Garth, K. R. Carter, *Polym. Degrad. Stab.* **2015**, *121*, 303 – 310; b) L. E. Ruff, E. A. Mahmoud, J. Sankaranarayanan, J. M. Morachis, C. D. Katayama, M. Corr, S. M. Hedrick, A. Almutairi, *Integr. Biol.* **2013**, *5*, 195 – 203.
[20] a) Y. Bae, S. Fukushima, A. Harada, K. Kataoka, *Angew. Chem. Int. Ed.* **2003**, *42*, 4640 – 4643; *Angew. Chem.* **2003**, *115*, 4788 – 4791; b) D. Chen, W. Liu, Y. Shen, H. Mu, Y. Zhang, R. Liang, A. Wang, K. Sun, F. Fu, *Int. J. Nanomed.* **2011**, *6*, 2053 – 2061.

[21] a) J. Liu, Y. Huang, A. Kumar, A. Tan, S. Jin, A. Mozhi, X. J. Liang, *Biotechnol. Adv.* **2014**, *32*, 693 – 710; b) F.-Q. Hu, Y.-Y. Zhang, J. You, H. Yuan, Y.-Z. Du, *Mol. Pharmacol.* **2012**, *9*, 2469 – 2478.
[22] S. Su, F.-S. Du, Z.-C. Li, *Macromolecules* **2018**, *51*, 6571 – 6579.
[23] E. Fleige, K. Achazi, K. Schaletzki, T. Triemer, R. Haag, *J. Controlled Release* **2014**, *185*, 99 – 108.
[24] M. R. Molla, T. Marcinko, P. Prasad, D. Deming, S. C. Garman, S. Thayumanavan, *Biomacromolecules* **2014**, *15*, 4046 – 4053.
[25] a) C. Wang, Q. Ge, D. Ting, D. Nguyen, H. R. Shen, J. Chen, H. N. Eisen, J. Heller, R. Langer, D. Putnam, *Nat. Mater.* **2004**, *3*, 190 – 196; b) J. Heller, A. C. Chang, G. Rood, G. M. Grodsky, *J. Controlled Release* **1990**, *13*, 295 – 302; c) D. Koylu, K. R. Carter, *Macromolecules* **2009**, *42*, 8655 – 8660; d) J. K. Varghese, N. Hadjichristidis, Y. Gnanou, X. Feng, *Polymer Chem.* **2019**, *10*, 3764 – 3771.
[26] a) D. Liu, C. W. Bielawski, *Macromol. Rapid Commun.* **2016**, *37*, 1587 – 1592; b) P. Lundberg, B. F. Lee, S. A. van den Berg, E. D. Pressly, A. Lee, C. J. Hawker, N. A. Lynd, *ACS Macro Lett.* **2012**, *1*, 1240 – 1243.
[27] M. Worm, D. Leibig, C. Dingels, H. Frey, *ACS Macro Lett.* **2016**, *5*, 1357 – 1363.
[28] a) M. R. Aguilar, A. Gallardo, M. d. M. Fernández, J. S. Román, *Macromolecules* **2002**, *35*, 2036 – 2041; b) A. Natalello, M. Werre, A. Alkan, H. Frey, *Macromolecules* **2013**, *46*, 8467 – 8471; c) J. Herzberger, K. Fischer, D. Leibig, M. Bros, R. Thiermann, H. Frey, *J. Am. Chem. Soc.* **2016**, *138*, 9212 – 9223.
[29] J. Blankenburg, E. Kersten, K. Maciol, M. Wagner, S. Zarbakhsh, H. Frey, *Polym. Chem.* **2019**, *10*, 2863 – 2871.
[30] H. Pohlit, I. Bellinghausen, M. Schömer, B. Heydenreich, J. Saloga, H. Frey, *Biomacromolecules* **2015**, *16*, 3103 – 3111.
[31] H. Pohlit, D. Leibig, H. Frey, *Macromol. Biosci.* **2017**, *17*, 1600532.
[32] a) E. Merrill, K. Dennison, C. Sung, *Biomaterials* **1993**, *14*, 1117 – 1126; b) L. M. Weber, C. G. Lopez, K. S. Anseth, *J. Biomed. Mater. Res. Part A* **2009**, *90*, 720 – 729.

Manuscript received: November 24, 2019
Accepted manuscript online: December 18, 2019
Version of record online: February 18, 2020

